Thermal Modeling for Predication of Automobile Cabin Air Temperature

S. Sanaye*,1 and M. Dehghandokht2

¹Associate Professor, ²Ph. D., Energy Systems Improvement Laboratory, Mechanical Engineering Department, Iran University of Science and Technology, Narmak, Tehran, Iran

Abstract

Thermal modeling of an automotive cabin was performed in this paper to predict the inside cabin air temperature. To implement this task, thermal and ventilation loads were estimated and the mass and energy balance conservation equations for dry air and water vapor with considering a new parameter (air circulation ratio) as well as the balance equations of internal components of a cabin were derived and solved simultaneously. The performance of the proposed thermal modeling of a cabin was compared with the data collected from hot room experimental tests. These tests were run for various design parameters such as evaporating cooling load and cabin size (air volume inside cabin). The comparison of experimental and numerical results showed a good agreement.

Parametric analysis with three parameters namely, vehicle speed, number of passengers, and A/C air mass flow rate was performed to investigate the effects of these parameters on cabin air temperature.

Keywords: Automobile cabin air temperature; thermal modeling; thermal loads; hot room test; evaporator capacity

1. INTRODUCTION

The combined application of analytical, numerical and experimental study of passenger compartments (cabins which are enclosed environments) of automobiles is important to improve the thermal comfort of passengers. In the United States, approximately 26 million liters of fuel are consumed annually for cooling vehicle passenger compartment [1] which can be reduced considerably by predicting inside cabin air condition before the final selection of components of air conditioning system and the final cabin design.

Many studies on the fluid and thermal characteristics of passenger compartments have been carried out using both experimental and numerical analysis. Kohler [2] investigated the variation of humidity and temperature with time for a bus with capacity of 50 persons. They integrated Lumped HVAC system simulation into their model. Reported predictions and experiments were in good agreement. Experiments were limited to a period of one hour in which the vehicle was at rest under dynamic solar loading. Eisenhour [3] described the in cabin heat flux with a steady state energy balance equation that accounted the thermodynamic interactions between the interior temperature, atmospheric temperature, and

the interior air flow.

Stancato [4] developed a simulation model to estimate the steady state heat loads in a cabin. The heat loads included solar radiation through glasses, conduction through the body walls and glasses, fresh air infiltration, as well as heat loads of passengers and equipment.

Huang and Han [5] presented a three-dimensional hot soak and cool-down transient analysis which took into accounts the glazed surfaces and pertinent physical and thermal properties of the enclosure for the passenger compartment. Kataoka and Nakamura [6] studied the flow and temperature fields of a passenger compartment including the operation of the cooling system, the heat transfer at the wall by solar radiation, and actual vehicle driving conditions. Chein [7] applied a numerical simulation to investigate the thermal behavior and comfort in a vehicle. The cooling capacity was computed using equations of å?-NTU (effective number of transfer units) method. The predicted temperature distribution in the passenger cabin of a vehicle was in good agreement with experimental results. Chao gang [8] proposed a model for vehicle climate control system which included air conditioning and engine cooling systems under different operational conditions. The performance of the vehicle system climate control was simulated, and

^{*} sepehr@iust.ac.ir

the modeling output was in good agreement with experimental data. Durovic [9] used artificial neural network under several weather conditions to control the temperature of a cabin. Shiming [10] analyzed the dynamic mode of refrigerating cycle to control the cabin thermal comfort. In his work, the moisture produced by passengers was measured by a sensor, while the governing equations were just applicable to 100% circulated return air passing over the evaporator.

In the first part of this paper, the thermal and ventilation loads were estimated, and then the balance equations of mass and energy for dry air as well as balance equations for internal components of a cabin were derived and solved simultaneously. proposed cabin thermal model was validated by hot room test experimental data. Then the parametric study was performed to investigate the factors which affect the temperature variations within the passenger compartment. Therefore the refrigeration cycle model and air cabin model were coupled to predict the effects of refrigeration cycle operation on the cabin air conditions. In the present cabin air temperature modeling, the air circulation ratio (the ratio of circulating air mass flow rate to the air mass flow rate flowing through evaporator) could be taken into account and the mass and energy balance equations for cabin air were derived with considering the effect of this parameter. Furthermore the analysis has been performed for our specific refrigeration cycle modeling which consists of specific compressor [11], evaporator and condenser [12] models. Finally the analysis was performed for specific atmospheric conditions (temperature, humidity and solar radiation) as well as our interested cabin geometry and specifications of cabin internal materials.

2. THERMAL MODELING AND GOVERNING EQUATIONS FOR AN AUTOMOBILE CABIN

The cabin thermal modeling was performed by using the Lumped Capacitance Method in which the temperature distribution was assumed to be uniform spatially [13]. This assumption implies complete mixing of air inside the cabin at all times. The variation of temperature and relative humidity of air inside the cabin was estimated using dynamic equations of operating conditions which were influenced by: solar radiation load received by outer surfaces and windows of automobile, convection and

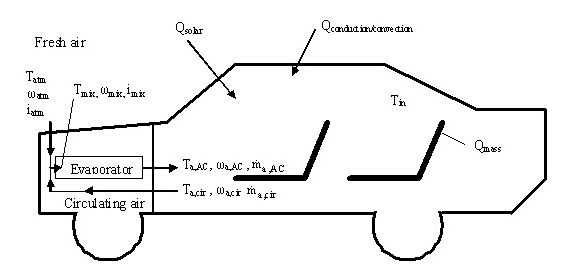


Fig. 1. The schematic diagram of cabin for an automobile

conduction heat transfer loads of cabin, effect of sensible and latent heats as well as the inlet cold air from the air conditioning system (Fig. 1). Therefore four nonlinear differential equations for the cabin air were constructed including mass balance of dry air (section 2.1), mass balance of water vapor (section 2.2), energy balance of inside air (section 2.3) and energy balance for the interior components of a cabin (section 2.4). These balance equations were from reference [13], however, they were modified to consider the effects of air circulation ratio as are explained in the following sections.

2. 1. Dry Air Mass Balance Equation in a Cabin

Considering the cabin of an automobile as a control volume, the following mass balance equation for the dry air was derived as:

$$\frac{d\mathbf{m}_{a}}{dt} = (1 - \zeta)\dot{\mathbf{m}}_{a,AC} + \dot{\mathbf{m}}_{a,inf} \tag{1}$$

where the ratio of mass flow rate of circulating air to the air flow rate passing through the evaporator is defined as the air circulation ratio (Fig.1):

$$\zeta = \frac{\dot{m}_{a,cir}}{\dot{m}_{a,\Delta C}} \tag{2}$$

The first term in left hand side (lhs) of Eq. 1 shows the transient change of air mass in the cabin. The first term in the right hand side (rhs) of Eq. 1 is the cabin inlet air mass flow rate passing through the evaporator ($\dot{m}_{a,AC}$). The second term in the rhs of Eq. 1 is the recirculation air mass flow rate ($\dot{m}_{a,cir} = \dot{m}_{a,AC}$. ξ) exiting from the control volume. The third term in the right hand side of Eq. 1 is the mass flow rate of infiltration air ($\dot{m}_{a,inf}$).

The cabin infiltration air passes through the gaps of doors and windows due to a slight vacuum pressure inside the compartment (for which there is not enough information in open literature to estimate this mass flow rate directly). It was assumed that the absolute humidity of infiltration air was the same as the humidity of the atmospheric air.

2. 2. Water Vapor Mass Balance Equation in a Cabin

The evaporator exit air (sum of inlet fresh air and the circulated air back into the evaporator inlet), have considerable amount of humidity which its level increases due to aspiration of passengers. Considering the cabin as a control volume, the mass balance equation for water vapor was derived in the following form:

$$\frac{d(m_a\omega)}{dt} = (\dot{m}_a\omega)_{inf} + (\dot{m}_a\omega)_{AC} + \dot{m}_{v,human} - (\dot{m}_a\omega)_{cir}$$
(3)

The (ℓ hs) term of Eq. 3 is the transient change of inside cabin water vapor mass, the first term in (rhs) of Eq. 3 is the infiltration water vapor mass flow rate $\dot{m} \omega$, the second term in (rhs) is the water vapor mass flow rate of air passing through the evaporator, the third (rhs) term is the water vapor produced by human aspiration and the fourth (rhs) term is the outlet water vapor mass flow rate from the cabin (by reciculating air).

As explained in the last paragraph of section 2.1, $\omega = \omega$

By substituting Eq. 1 into the lhs term of Eq. 3, the mass conservation equation for water vapor content of air in a cabin was obtained as:

$$\frac{d\omega}{dt} = \frac{\dot{m}_{a,AC} \left[\omega_{AC} - \omega\right] + \dot{m}_{a,inf} \left[\omega_{atm} - \omega\right] + \dot{m}_{v,humar}}{m_a} \tag{4}$$

2. 3. Energy Conservation Equation for the Air in a Cabin

Considering cabin as a control volume, energy balance for the air in cabin would be:

$$\frac{d(m_a i)}{dt} = \sum \dot{Q} + (\dot{m}_{a,AC} i_{AC}) + (\dot{m}_{inf} i_{inf}) - (\dot{m}_{a,cir} i_{cir})$$
(5)

The cabin air thermal loads have three main sources: solar thermal load passing through windows and bodywork of vehicle ($\mu\dot{Q}_{solar}$), thermal load of convection (\dot{Q}_{conv}) and conduction (\dot{Q}_{cond}) heat

transfer from bodywork of the vehicle and the thermal load of passengers (\dot{Q}_{human}), then:

$$\sum \dot{Q} = \mu . \dot{Q}_{solar} + \dot{Q}_{human} + \dot{Q}_{cond} + \dot{Q}_{conv} + \dot{Q}_{mas} \tag{6}$$

In Eq. 6 \dot{Q}_{mass} is the heat transfer rate between air and internal components in cabin which may be estimated from \dot{Q}_{mass} = h . A_{mass} .(T_{mass} - T_{in}). The parameter μ in Eq. 6 is a weighting parameter to indicate the fraction of solar load which was absorbed by the air in cabin. Therefore $(1-\mu)$ \dot{Q}_{solar} was absorbed and dissipated by cabin internal components. By substituting Eq 1 in the (ℓ hs) of Eq. 5, the energy conservation equation for the air in cabin was finally obtained from:

$$\frac{\mathrm{di}}{\mathrm{dt}} = \frac{\sum \dot{Q} + \dot{m}_{a,AC} [\dot{i}_{AC} - \dot{i}] + \dot{m}_{a,inf} [\dot{i}_{atm} - \dot{i}]}{m_a}$$
(7)

2. 4. Energy Balance for the Internal Components of a Cabin

To account for the heat capacity of internal components of cabin acting as a heat source or heat sink which transfer heat to the air, a lumped mass was used to represent all the cabin internal components. Considering internal components of cabin as a control volume then [13]:

$$(1-\mu)\dot{Q}_{solar} - \dot{Q}_{mass} = (mc)_{mass} \frac{dT_{mass}}{dt}$$
 (8)

Replacing \dot{Q}_{mass} in Eq. 8 by its definition (\dot{Q}_{mass} = h.A_{mass}·(T_{mass} - T_{in})), the equation for temperature variation of cabin internal components was obtained as:

$$\frac{dT_{mass}}{dt} = \frac{(1-\mu)\dot{Q}_{solar} - h \cdot A_{mass} \cdot (T_{mass} - T_{in})}{m_{mass}c_{mass}}$$
(9)

Eqs. (1), (4), (7) and (9) are four mass and energy balance differential equations which were solved to find m_a (cabin air mass), ω (cabin air humidity), i (cabin air enthalpy), T_{mass} (interior mass temperature).

2. 5. Thermal Analysis of Air Passing Through the Evaporator

 i_{AC} and ω_{AC} which are needed in Eqs. 7 and 4 respectively were estimated by knowing the cooling capacity \dot{Q}_{evap} (which was obtained from the model of

refrigeration cycle). By considering the evaporator as a control volume, and by applying water vapor mass and energy balance equations for humid air passing through the evaporator (Fig. 1), i_{AC} and ω_{AC} then were obtained from the following conservation equations:

$$\dot{\mathbf{m}}_{\mathbf{a},\mathbf{AC}}\boldsymbol{\omega}_{\mathbf{mix}} = \dot{\mathbf{m}}_{\mathbf{a},\mathbf{AC}}\boldsymbol{\omega}_{\mathbf{AC}} + \dot{\mathbf{m}}_{\mathbf{W}} \tag{10}$$

$$i = i - \frac{\dot{Q}}{\dot{m}} - \frac{\dot{m} i}{\dot{m}}$$
 (11)

 $\dot{m}_{\rm w}$ is the condensed water vapor in evaporator (drain) when humid air passes through its cooling surface. $i_{\rm mix}$ and $\omega_{\rm mix}$ in Eqs 10 and 11 are the enthalpy and absolute humidity of inlet air into the evaporator (after mixing the fresh air and the circulating air, Fig. 1). These parameters were obtained by applying the conservation equation of mass for water vapor and the conservation equation of energy for mixing air process at the evaporator inlet:

$$\omega_{\text{mix}} = \frac{\zeta \cdot \dot{m}_{a,\text{AC}} \cdot \omega_{\text{cir}} + (1 - \zeta) \dot{m}_{a,\text{AC}} \cdot \omega_{\text{out}}}{\dot{m}_{a,\text{AC}}}$$
(12)

$$i_{mix} = \frac{\zeta.\dot{m}_{a,AC}.\dot{i}_{cir} + (1 - \zeta)\dot{m}_{a,AC}.\dot{i}_{out}}{\dot{m}_{a,AC}}$$
(13)

3. MODELING THE THERMAL LOADS OF AIR IN A CABIN

The cabin of automobiles are exposed to the transient environmental conditions which change the thermal loads of solar radiation, conduction and convection heat transfer rates as well as the thermal load for passengers. Fig. 1 shows the schematic diagram of a cabin and its thermal loads.

3. 1. The Solar Thermal Load

The solar thermal load for a cabin was estimated from HDKR [14] homogenous model. The total absorbed solar energy by the cabin surfaces is explained as follows [15]:

$$G = G \cdot R + G \cdot \left[\frac{1 + \cos \beta}{2}\right] + \rho \cdot \left[G + G \cdot \right] \left[\frac{1 + \cos \beta}{2}\right] + G \tag{14}$$

where the total solar thermal load for cabin was estimated from:

$$\dot{Q}_{\text{solar}} = G_{\text{total}} \tau_{\text{s}} A_{\text{win}} \tag{15}$$

Q_{solar} includes solar thermal loads absorbed from the total window surface area including rear window, windshield and side windows as follows:

$$\dot{Q}_{\text{solar}} = \dot{Q}_{\text{front,win}} + \dot{Q}_{\text{rear,win}} + \dot{Q}_{\text{side,wins}}$$
 (16)

3. 2. The Convection and Conduction Heat Transfer Thermal Loads

The magnitude of convection thermal load depends on internal and external surface positions, ambient temperature as well as the vehicle speed (or air speed). Assuming a warmer air in surrounding environment, the following heat transfer mechanisms occur [16]:

- a) The forced convection heat transfer between ambient warm air and the external cabin surface.
- b) The conduction heat transfer between interior and exterior layers with the air gap in between.
- c) The natural convection heat transfer between interior surfaces of the cabin and the conditioned (cool) air in cabin.

The amount of the above mentioned loads depend on the boundary conditions such as automobile interior and exterior surface temperatures, air velocity and solar load. Therefore for cabin convection and conduction load analysis the cabin was divided into six separate sections included windshield, rear window, side windows, doors, roof and floor. For each above mentioned sections the effective parameters such as air velocity, temperature, material specifications, slope and type of material were collected.

In estimating the thermal loads resulting from convection and conduction heat transfer, the typical equivalent thermal resistance between outside and inside temperatures was applied as is shown in Fig. 2.

By considering the radiation absorbed by exterior

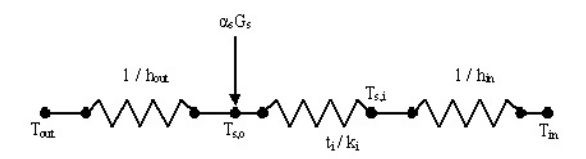


Fig. 2. Equivalent thermal resistance of bodywork for an automobile

surfaces, the thermal balance at a point (node) with $T_{s,o}$ temperature (at exterior surface of the vehicle) may be expressed as:

$$q''_{conv,out} + \alpha_S G_S = q''_{cond}$$
 (17)

Alternatively in an equivalent form:

$$h_o(T_{out} - T_{s,o}) + \alpha_s G_s = \frac{T_{s,o} - T_{s,i}}{\sum \frac{x_i}{k_i}}$$
 (18)

where h_o is the outside air heat transfer coefficient.

From the energy balance at node with $T_{s,i}$ temperature, then:

$$q''_{cond} = q''_{conv} \tag{19}$$

or in an equivalent form:

$$\frac{T - T}{\sum \frac{x}{k}} = \frac{T - T}{\frac{1}{h}} \tag{20}$$

where q''_{conv} is the heat flux exchanging between vehicle exterior surface metal (with $T_{s,o}$ temperature) and the ambient air temperature (T_{out}) .

The outside air forced convection heat transfer coefficient ho for horizontal exterior surfaces (cabin roof and floor) was estimated from the following empirical equation [16]:

$$Nu = \begin{bmatrix} 0.037 (Re) & 1 \end{bmatrix} (Pr)$$
 (21)

For the natural convection on horizontal internal surfaces such as roof, air in cabin is under the surface, hence, the temperature of roof is higher than the air in cabin, then for surfaces heated from the above [16]:

$$Nu = 0.27Ra^{1/4} \tag{22}$$

and for the natural convection on horizontal internal surfaces such as cabin floor, for which air in cabin is above the floor and its temperature is lower than the floor, Nu was estimated from [16]:

$$Nu = \begin{cases} 0.54Ra^{1/4} & 10^4 \le Ra \le 10^7 \\ 0.15Ra^{1/3} & 10^7 \le Ra \le 10^{11} \end{cases}$$
 (23)

For the natural convection on inclined surfaces

such as wind screen shield and rear window:

For Ra $> 10^9$:

$$Nu = \begin{cases} 0.825 + \frac{0.387(Ra)}{\left[1 + \binom{0.429}{Pr}\right]} \end{cases}$$
 (24)

And for $Ra < 10^9$:

Nu = 0.68 +
$$\frac{0.67 \text{Ra}_{L}^{1/4}}{\left[1 + \left(0.492 / \text{Pr}\right)^{9/16}\right]^{4/9}}$$
 (25)

3. 3. The Sensible and Latent Loads of Passengers

The human thermal load was estimated from [17]:

$$\dot{Q}_{human} = np(SH + LH)$$
 (26)

where, np is the number of passengers, SH is sensible heat and LH is latent heat for the light activity (sitting situation for passengers).

Furthermore there is an increase in humidity produced by passengers due to three factors of m_{res} , m_{sw} and m_{diff} :

m_{res} is the respiration factor which is a function of metabolic rate (M) and was obtained from the following experimental relation [18]:

$$\dot{m}_{res} = 0.43 \times 10^{-6} \left(\frac{\text{kg.m}^2}{\text{J}} \right) M$$
 (27)

where M was considered to be 1640 (J/m².s).

 \dot{m}_{sw} is directly proportional to the latent thermal losses from skin, related to the body temperature regulating mechanism, this parameter was estimated from:

$$\dot{m} = \frac{E}{\dot{i}} \tag{28}$$

where the latent thermal losses from skin (sweating thermal load, E_{sw}) was computed from [19]:

$$E_{sw} = 0.07 (M - 58.12).A_D$$
 (29)

 $\dot{m}_{\rm diff}$ is the spread water vapor mass flow rate from skin, determined by diffusive thermal load $E_{\rm diff}$, divided by latent heat of saturated water at the skin

temperature (i_{fg}):

$$\dot{\mathbf{m}} = \frac{\mathbf{E}}{\mathbf{i}} \tag{30}$$

The procedure of computing E_{diff} , requires some input parameters obtained from experimental data such as thermal resistance of cloths (I_{cl}), vaporizing heat transfer coefficient, and perspiring rate. A proposed equation for computing E_{diff} is [19]:

$$E_{diff} = 0.508 \times 10^{-3} (p_{wl} - p_{wa}).A_{D}$$
 (31)

where p_{wa} is the corresponding saturated pressure of water vapor at cabin air temperature, and p_{wl} is the corresponding saturated pressure of water vapor at skin temperature derived from:

$$p_{wl} = 256T_{sk} - 3373 \tag{32}$$

where T_{sk} is the skin temperature of one person which has the following relation with the metabolic rate of that passenger:

$$T_{sk} = 35.7 - 0.02275M \tag{33}$$

In case of existing perspiring rate and ambient temperature in vicinity of human thermal comfort zoon, it could be assumed that the perspiration would be totally vaporized. Hence, the resultant equation for estimating the water vapor produced by passengers is:

$$\dot{\mathbf{m}}_{v,\text{human}} = \mathbf{np} \times (\dot{\mathbf{m}}_{\text{res}} + \dot{\mathbf{m}}_{\text{sw}} + \dot{\mathbf{m}}_{\text{diff}}) \tag{34}$$

The humidity load from passengers increases the relative humidity of air in cabin and may cause a non-comfort air condition in cabin which should be taken care of by the cabin air-conditioning system.

4. SOLVING THE SYSTEM OF GOVERNING CONSERVATION EQUATIONS

Four coupled nonlinear ordinary differential equations including Eq. 1 (for mass conservation of dry air in cabin), Eq. 4 (for water vapor mass conservation for air in cabin), Eq. 7 (energy balance for air in cabin) and Eq. 9 (for energy balance of internal components in the cabin), constructed the lumped system model of analysis for the cabin air. Four differential equations were solved simultaneously using a classical fourth-order Runge-kutta method to obtain the variation of dry air mass absolute humidity, enthalpy, and temperature of air in cabin at each time step.

The relations of absolute humidity with temperature for air in cabin are as follows:

$$T_{\rm in} = \frac{i - 2501.\omega}{1.006 + 1.805\omega} \tag{35}$$

where i is the enthalpy of air in cabin.

5. THE CASE STUDY AND THE OPERATING CONDITIONS

In order to analyze and evaluate the accuracy of results for the proposed cabin thermal model, an automobile with the characteristics of its cabin and air conditioning system components shown in Table 1 was selected.

For comparison of simulation/modeling results and the corresponding experimental results the experimental hot room tests were performed. In these tests the atmospheric and thermal conditions for automobile and its cabin at various speeds were adjusted similar to that of the actual case for performing the tests. For example various vehicle speeds were obtained by blowing air over

Table 1. The geometrical specifications of components for an automobile in hot room test

Title	Туре	Geometry
Compressor displacement volume	Rotary vane	120 cc
Condenser	Parallel flow	545 mm × 319 mm × 16 mm
Expansion valve	Thermostatic expansion	
Evaporator sizes	Laminated	208 mm × 195 mm × 95 mm
Engine displacement volume		1300 cc
Cabin sizes		2300 mm × 1300 mm × 1190

Items	Scale	Precision
Vehicle speed	0-120 (km/h)	±0.1 (km/h)
Atmospheric temperature	0-60 (°C)	±1 (°C)
Sunlight power	0- 1200 (W/m)	
Air velocity	0-120 (km/h)	±1 (km/h)
Thermocouple	0-60 (°C)	±0.1 (°C)
Pressure transducer	0.8-35 (bar)	±0.1 (bar)

Table 2. The accuracy of experimental parameters

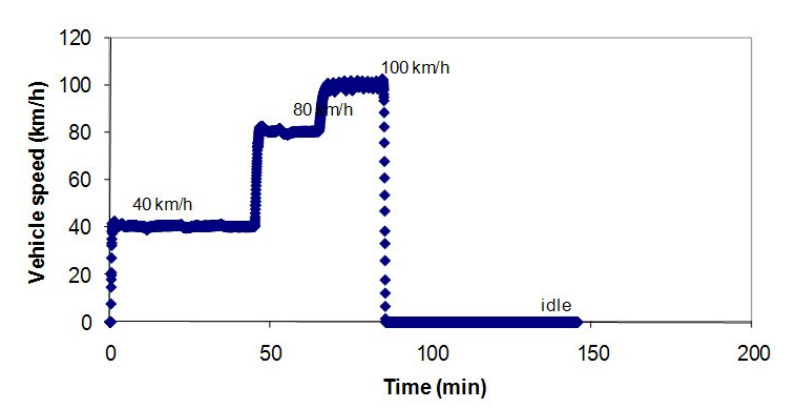


Fig. 3. Modeling and hot room test condition

the vehicle at various air speeds. Automobile speeds followed the standard time line events during gathering experimental data. Fig. 3 shows the followed time line events. At time zero, the vehicle began to move at the speed of 40 km/h during the first 45 minutes. In the next step the speed increased to 80 km/h in the next 20 minutes. Then the speed increased further up to 100 km/h in the next 20 minutes before running at the idle

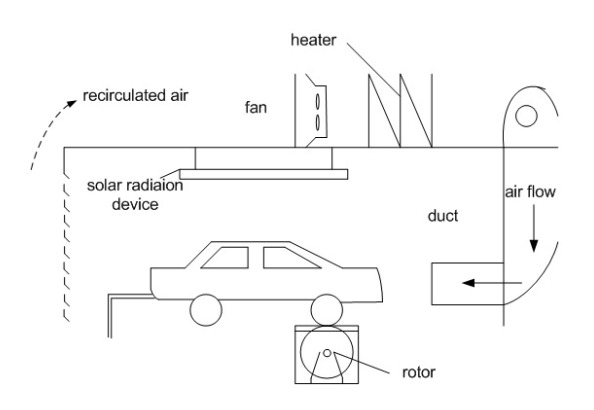


Fig.4. The schematic diagram of a hot room test

(zero speed) mode for the final 30 minutes. Furthermore 1200 watts radiating heating panels on the test section ceiling provided the sun radiation heat transfer load. With these panels the cabin air temperature reached 60 °C (mentioned in standards while the ambient temperature was held constant at 43 °C during the experiments). There were temperature sensors inserted at various locations of cabin inside to measure the cabin mean temperature. There were also pressure and temperature sensors to measure the operating conditions of the components in compression refrigeration cycle. Fig. 4 shows the schematic diagram of hot room test section for performing the experiments. The measured parameters and their accuracy are shown in Table 2.

6. DISCUSSION AND RESULTS

6. 1. Model verification

In order to verify the numerical results of the simulation model, a real automobile with specifications introduced in section 5 and Table 1 was tested at the described operating condition.

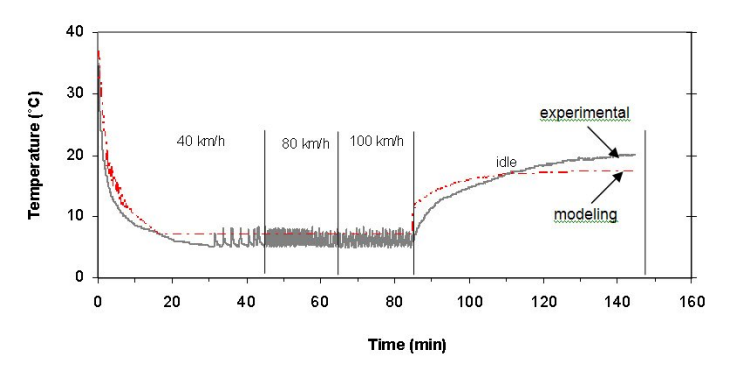


Fig. 5. A/C outlet air temperature for the case I (4100 W) tested evaporator

Fig. 5 compares the predicted modeling airconditioning (A/C)outlet temperature values (evaporator exit air temperature) with corresponding experimental data as a function of time. After starting and running the A/C system, as time passed on, the A/C (evaporator) outlet temperature dropped with an average difference value of 1.2 °C between modeling and experimental results during first 15 minutes. Then it reached a steady state value (with 1 °C average difference) in the time interval of 15 to 80 minutes. After 85 minutes, the speed decreased abruptly to zero. This was a sudden rise in A/C outlet temperature because there was not sufficient supplied cooling capacity by evaporator due to omitting the forced convection heat transfer and rejecting heat by that mechanism when the vehicle stopped. The average of difference values between modeling and experimental data for time interval of 85 to 115 and 115 to 145 minutes were 1.18 and 1.67 °C respectively. The above temperature difference values were partly related to the modeling of the refrigeration cycle and components.

Oscillations of cabin air temperature with time during 30 to 85 minutes for experimental data were due to setting the evaporator air temperature at a specific value (5 °C). For adjusting this temperature, the compressor of refrigeration system was shut down by thermostat and this procedure occurred repeatedly during 30 to 85 minutes. The adjusted evaporator exit air temperature was also an input to the modeling code. When the evaporator exit air temperature became lower than that value, the temperature setting value was considered as the evaporator exit air temperature meaning that refrigeration system was shut down by thermostat.

Fig. 6 shows the cabin air temperature variation with time. In the first 10 minutes of starting period there was about 3.39 °C average difference value between modeling and experimental cabin air temperatures mainly due to the outlet air temperature difference in experimental and modeling results. In the time interval of 15 to 85, the air temperature reached a steady state value (with 0.5 °C average difference).

Due to decreasing the vehicle speed from 100

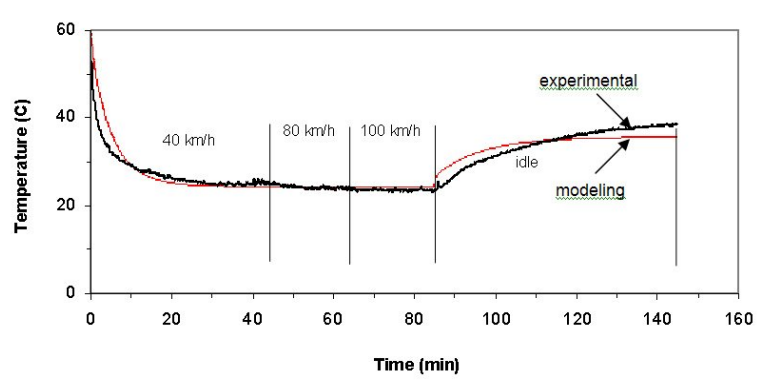


Fig. 6. Cabin average air temperature for the case I (4100 W) tested evaporator

km/hr to zero (idle) after 85 minutes, for omitting the forced convection heat transfer which provided partial heat rejection of the cabin air, and for lacking of sufficient cooling capacity, the air temperature of cabin increased abruptly. This resulted 3 °C difference value between modeling and experimental data at the beginning of idle (85 minutes) condition with average difference value of 1.27 °C during first 30 minutes of idling period.

One reason of this difference was due to the fact that after 85 minutes from the starting point, it took about one minute for decreasing the vehicle speed from 100 km/h to zero (idle condition) in the hot room test. This is while that idling started exactly at 85 minutes in modeling computations which resulted higher temperature values for modeling results. At the end of the idling period (about 115 minutes after starting), the situation became inverse and the modeling temperature in Fig. 6 was lower than the corresponding experimental values with 1.93 °C average difference value.

The above difference values between modeling and experimental results showed that the cabin air temperature modeling was reliable and could be used to investigate the effect of design parameters on the air cabin temperature.

6. 2. Analysis of Design Parameters

Cabin size (air volume) and A/C (evaporator) cooling capacity are two important parameters in automotive refrigeration system design and selection. The effects of these two parameters on cabin air

temperature were investigated by the proposed thermal modeling.

The cabin size (cabin air volume)

The cabin size (volume) is an important factor in predicting the cabin air temperature. The variation of cabin air temperature with time for two different cabin air volumes is shown in Fig. 7. Due to increasing the cabin air volume, the geometrical specifications of door, windows and inside cabin parts changed for investigating the size increase.

This resulted in increasing the solar and convection loads as well as higher cabin air temperature for a fixed evaporator heat capacity.

Evaporator cooling capacity

Evaporator cooling capacity is also another important design parameter in selecting the automotive refrigeration system and reaching the required cabin air temperature during a permitted time period. The variation of cabin air temperature with time during idling period, for a specific cabin volume and various evaporator cooling capacities is shown in Fig. 8. With increasing the evaporator cooling capacity, the cabin air temperature decreases more rapidly. By using an evaporator (called case II) with 20% increased in cooling capacity in comparison with evaporator case I (with 4100 W cooling capacity), the cabin air temperature was about 3 °C colder at 30 minutes after starting point.

These results may be used to check whether the

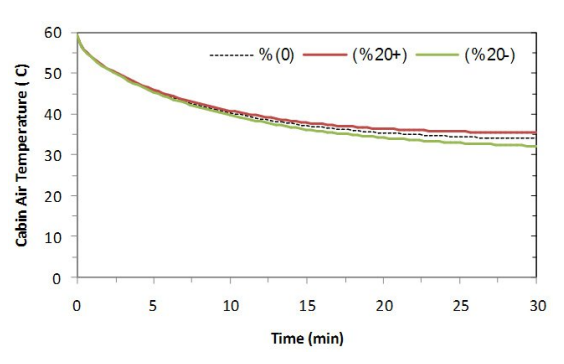


Fig. 7. Variation of cabin air temperature with time for various cabin air volumes (modeling results) for the case I (4100 W) tested evaporator during idling condition

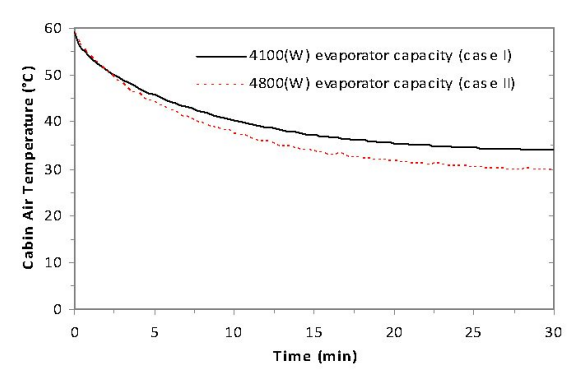


Fig. 8. Variations of cabin air temperature with time for various values of evaporator capacities during idling condition

designed A/C system was able to decrease the cabin air temperature after a specific time interval to or less than the specific required value. This fact should be taken care of in automobile system A/C design, testing, and operation standards.

Air circulation ratio

The air recirculation ratio is one of important design parameters in predicting the cabin air temperature. The variation of cabin air temperature with time for two different air circulation ratios and is shown in Fig. 9. With increasing the circulation ratio, the cabin air temperature decreases faster than that when more fresh atmospheric air inters the cabin (lower circulation ratio) during a specific operating time period. For example the cabin air temperature after running at idle condition for 30 minutes when was about 5 °C colder than when .

6. 3. Parametric Analysis

The simulation model was used to study the effects of certain vehicle and air conditioning parameters on the cabin air temperature. Three parameters namely, vehicle speed, number of passengers, and A/C mass flow rate were investigated.

Vehicle speed

Fig. 10 shows variation of cabin air temperature for 40 km/hr, 80 km/h, 100 km/h and idle (zero) speeds with time. As was expected for 40 km/hr vehicle speed, the cabin air temperature was lower than the

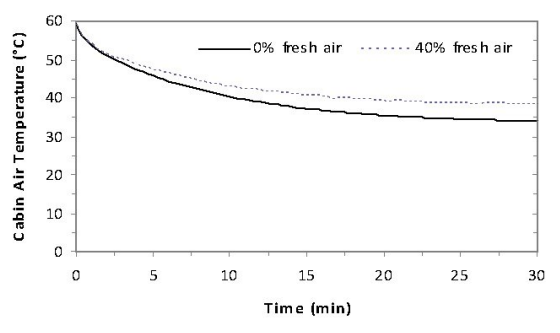


Fig. 9. Variation of cabin air temperature at two conditions: 0% and 20% fresh air for the evaporator Case I (4100 W) during idling condition

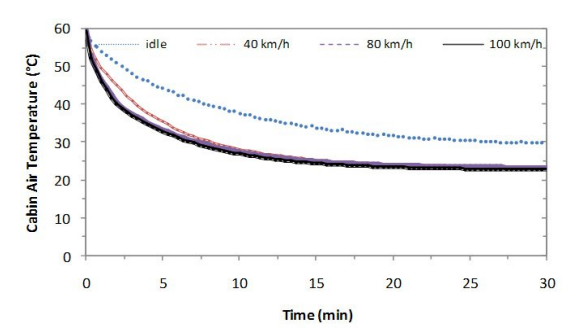


Fig. 10. Variation of cabin air temperature with time for various vehicle speeds (modeling results) for the case II (4800 W) evaporator

idling operation mode throughout the test. This occurred due to omitting the cabin air heat rejection by convection heat transfer mode during idling running period. Furthermore due to lower compressor speed during idling operating mode, lower values of refrigerant mass flow rate passed through the evaporator.

With increasing the vehicle speed from 40 to 80 km/hr and then from 80 to 100 km/h, there was no significant change in cabin conduction and convection heat transfer rate. Therefore no significant change in cabin air temperature was obtained as shown in Fig. 10. For all 40, 80 and 100 km/hr cases, the cabin air temperature reached the required (adjusted) value (23 °C) in 15 minutes.

Number of passengers

By increasing the number of passengers, the time interval for reaching the adjusted cabin air temperature was shorter (faster temperature decrease) due to smaller air volume (and mass). The variation of cabin air temperature with time during idling running period, for a specific cabin volume and various number of passengers is shown in Fig. 11. By increasing the number of passengers to 4, the cabin air temperature was about 2 °C colder at 30 minutes after initial A/C starting.

A/C air mass flow rate

Fig. 12 shows the variation of cabin air temperature with time during idling period, for a specific cabin air mass flow rate (360 kg/hr) as well as 20% increase in the amount of A/C air mass flow rate. By increasing

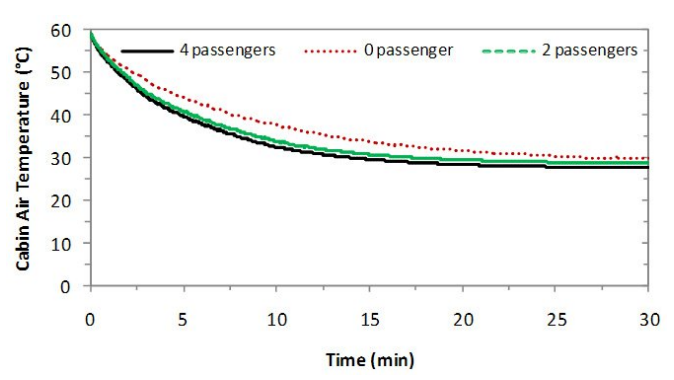


Fig. 11. Variation of cabin air temperature with time for various number of passengers (modeling results) for the case II (4800 W) evaporator during idling condition

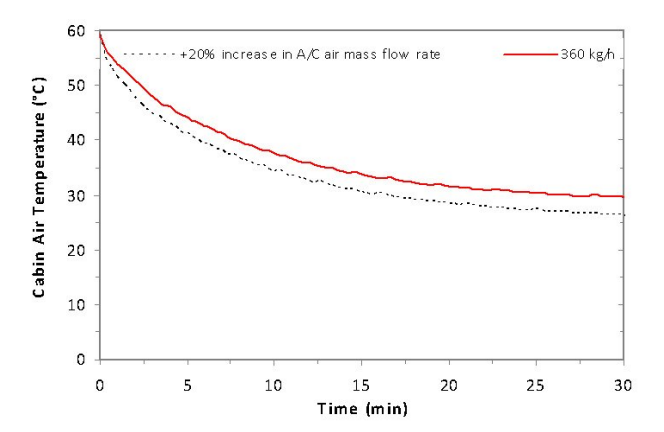


Fig. 12. Variation of cabin air temperature with time for various A/C air mass flow rates (modeling results) for case II (4800 W) evaporator during idling condition

the A/C air mass flow rate for 20%, the cabin air temperature was about 3 °C colder at 30 minutes after initial A/C starting. Therefore using a larger blower (increase in air mass flow rate) decreased the cabin air temperature in a shorter time period. However, noise and vibration induced by a larger blower should be taken into account and consideration.

7. CONCLUSION

Thermal modeling of cabin air temperature in an automobile was performed here. A new parameter (air circulation ratio) was defined and considered in our modeling and analysis. Therefore the mass and energy balance equations were derived showing the effect of this parameter on conservation equations. The proposed model was validated with experimental data. The modeling results showed a good agreement with the experimental hot room test data. The thermal modeling

supports designers for choosing an appropriate evaporator heat capacity (with suitable actual heat duty) for vehicles with various cabin sizes. It would be also applicable to estimate the cabin air temperature in various operating conditions. The modeling results showed that with increasing/decreasing the cabin size (air volume inside cabin) for 20%, and after 20 minutes of running air conditioning system, the cabin air temperature increased/decreased 1.2 and 1.5 °C respectively in comparison with the cabin temperature of our case study. Furthermore with increasing the cooling capacity of evaporator for 20%, the cabin air temperature decreased (4 °C) in comparison with the cabin temperature of the investigated case study after 30 minutes of running air conditioning system in idling engine operation mode. It was observed that the parameters such as vehicle speed, number of passengers, and A/C air mass flow are important to predict the cabin air temperature. Parametric analysis demonstrated that our developed model may be used for automobile A/C design purposes with the advantages of cost and time savings. It also helps users to investigate how various factors affect the air cabin temperature without involving and performing the expensive and time consuming experimental tests.

REFERENCES

- Rugh, J. P., Farrington, R., Bharathan, D., [1] Vlahinos, A., Burke, R., Huizenga, C., and Zhang, H., "Predicting human thermal comfort transient nonuniform thermal environment", In Proceedings of the Fifth International Meeting on Thermal Manikins and Modeling, 5IMM, Strasbourg, France, 2003 (National Institute for Working Stockholm, Sweden), also in Eur. J. Appl. Physiol., 2004, Vol. 92, No. 6, 721-727.
- [2] Kohler, J., Kuhn, B., Sonnekalb, M., Beer, H., "Numerical Calculation of the Distribution of Temperature and Heat flux in Buses under influence of the vehicle Air Conditioning System", ASHRAE Trans, 1990, Vol. 96, part 1, 432-446.
- [3] Eisenhour, R., "Automatic Climate Control Equation for Improved Heat Flux Response", 1996, SAE paper 960683.
- [4] Stancato, F., Onusic H., "Road Bus Heat Loads Numerical and Experimental Evaluation", 1997, SAE Paper 971825.
- [5] Huang, T. L. and Han, T., "Validation of 3-D passenger compartment hot soak and cool-down analysis for virtual thermal comfort engineering", 2002, SAE Paper No. 2002-01-1304.
- [6] Kataoka, T. and Nakamura, Y., "Prediction of thermal sensation based on simulation of temperature distribution in a vehicle cabin", Heat Transfer-Asia Research, 2001, Vol. 30, 195-209.
- [7] Chien, C.-H., Jang, J.-Y., Chen, Y.-H., and Wu, S.-C., "3-D numerical and experimental analysis for airflow within a passenger compartment", International Journal of Automotive Technology, 2008, Vol. 9, No. 4, 437-445.
- [8] Zhao-gang, Q., Chen, J. P., Chen, Zhi-jiu., "Analysis and simulation of mobile air

- conditioning system coupled with engine cooling system Energy Conversion and Management", 2007, Vol. 48, Issue 4, 1176-1184.
- [9] Durovic, H.M., KovaZevic, B.D., "Control of heating, ventilation and air conditioning system based on neural network", in: 7th IEEE Seminar on Neural Network Application in Electrical Engineering, 2004.
- [10] Deng, Qi Qi, Shiming., "Multivariable controloriented modeling of a direct expansion (DX) air conditioning (A/C) system", International Journal of Refrigeration, 2008, Vol. 31, Issue 5, 841-849.
- [11] Sanaye, S., Dehghandokht, M., "Modeling of rotary vane compressor applying Artificial Neural Network", International Journal of Refrigeration, 2011, Vol. 34, 764-772.
- [12] Sanaye, S., Dehghandokht, M., "Modeling and Multi-objective optimization of parallel flow condenser using evolutionary algorithm", Applied Energy, 2011, 88, 1568-1577.
- [13] Yang, S.L., Arci, O., Huang, D.C., "A dynamic computer aided engineering model for automobile climate control system simulation and application, part 2: Passenger compartment simulation and application", SAE paper, 1999, No. 1990-01-1196.
- [14] Duffie, J.A., Beckman, W.A., "Solar Engineering of Thermal Processes" 2nd Edition, John Wiley & Sons, Inc, 1991.
- [15] Reindl, D.T., Beckman, W.A., and Duffie, J.A., "Evaluation of hourly tilted surface radiation models", Solar Energy 45, 1990, 9–17.
- [16] Incorpera, F.P., & Dewitt, D.P., "Introduction to Heat Transfer" John Willey and Sons. 1985.
- [17] Chan, A.S., "Cooling Load Calculation", the 4th International Conference on Indoor Air Quality, Ventilation and Energy Conservation in Buildings, Oct 2001.
- [18] Fanger, P.O., "Thermal Comfort", McGraw-Hill, Inc, 1970.
- [19] ASHRAE HANDBOOK, "Fundamentals" Atlanta, GA 30329, 2001.

NOMENCLATURE

A (m²) Surface area

A_D (m ²)	Skin surface area
c _{mass} (J/kg.K)	Specific heat of internal
	component
$E_{diff}(W)$	Diffusive thermal load
$E_{sw}(W)$	Sweating thermal load
G_{cb} (W/m ²)	Beam solar radiation
G_{cd} (W/m ²)	Diffuse solar radiation
G_{cr} (W/m ²)	Reflection solar radiation
$h (W/m^2.K)$	Heat transfer coefficient
I_{cl}	Thermal resistance of
	clothes
i (kJ/kg)	Enthalpy
i _{fg} (kJ/kg)	Latent heat of saturated water at the
	skin temperature
k (W/m.K)	Thermal conductivity
L_{H}	Latent heat
l_{hf}	Left hand side
m (kg)	Mass

MASS FLOW RATE

Metabolic rate
Number of passengers
Nusselt number
Pressure
Saturated pressure of vapor at skin
temperature
Saturated pressure vapor
Prandtl number
Heat transfer flux
Heat transfer rate
Ratio of beam radiation on a tilted
surface to that on horizontal surface
Raleigh number
Reynolds number
Right hand side
Sensible heat
Temperature
Thickness

Greek Letters

ζ		Circulation ratio
ω	(kgH O/kg dry	air) Absolute humidity
		or humidity ratio
ρ	(kg/m^3)	Density
μ		Weighting parameter
В		Angle

 au_{ss} Absorption coefficient au_{s} Transmission coefficient

Subscripts

Air

a

AC

atm	Atmosphere	
W	Water	
evap	Evaporator	
conv	Convection	
S	Surface	

s Surface
comb Combination
cond Conduction
i Inlet
in Interior
mass Internal components

Mixture mix Window win Respiration res Sweating sw diff Diffusive skSkin Vapor \mathbf{v} Circulation cir Infiltration inf

Air conditioning